

UC Santa Barbara

UC Santa Barbara Previously Published Works

Title

Simple Benchtop Approach to Polymer Brush Nanostructures Using Visible-Light-Mediated Metal-Free Atom Transfer Radical Polymerization

Permalink

<https://escholarship.org/uc/item/22x84514>

Journal

ACS Macro Letters, 5(2)

ISSN

2161-1653

Authors

Discekici, Emre H
Pester, Christian W
Treat, Nicolas J
[et al.](#)

Publication Date

2016-02-16

DOI

10.1021/acsmacrolett.6b00004

Peer reviewed

Simple Benchtop Approach to Polymer Brush Nanostructures Using Visible-Light-Mediated Metal-Free Atom Transfer Radical Polymerization

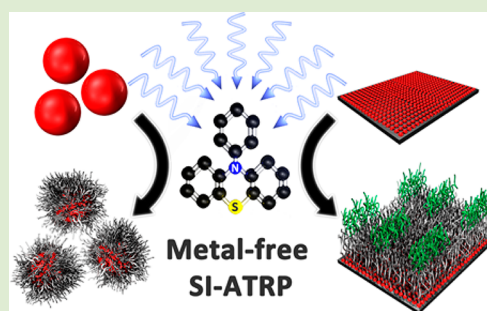
Emre H. Discekici,^{†,‡} Christian W. Pester,[‡] Nicolas J. Treat,^{‡,§} Jimmy Lawrence,[‡] Kaila M. Mattson,^{†,‡} Benjaporn Narupai,^{†,‡} Edward P. Toumayan,^{‡,⊥} Yingdong Luo,^{†,‡} Alaina J. McGrath,[‡] Paul G. Clark,^{||} Javier Read de Alaniz,^{*,†,‡} and Craig J. Hawker^{*,†,‡,§}

[†]Department of Chemistry and Biochemistry, [‡]Materials Research Laboratory, [§]Materials Department, and [⊥]Department of Chemical Engineering, University of California, Santa Barbara, California 93106, United States

^{||}The Dow Chemical Company, Midland, Michigan 48674, United States

Supporting Information

ABSTRACT: The development of an operationally simple, metal-free surface-initiated atom transfer radical polymerization (SI-ATRP) based on visible-light mediation is reported. The facile nature of this process enables the fabrication of well-defined polymer brushes from flat and curved surfaces using a “benchtop” setup that can be easily scaled to four-inch wafers. This circumvents the requirement of stringent air-free environments (i.e., glovebox), and mediation by visible light allows for spatial control on the micron scale, with complex three-dimensional patterns achieved in a single step. This robust approach leads to unprecedented access to brush architectures for nonexperts.



Surface-initiated polymerizations are a powerful and widely utilized approach to the preparation of robust and functional polymer surfaces.¹ Significant advances in this area have been enabled by the development of controlled radical polymerization strategies, including nitroxide-mediated polymerization (NMP),² reversible addition–fragmentation chain transfer polymerization (RAFT),³ and atom transfer radical polymerization (ATRP).⁴ These methods allow a wide variety of brush structures with controllable thickness and composition, including block copolymer structures, to be prepared.⁵ Access to these diverse architectures has led to numerous applications in areas such as antifouling coatings,^{6–8} drug delivery,⁷ stimuli-responsive materials,⁹ and nanoporous membranes.¹⁰

Until recently, the fabrication of patterned polymer brushes has required advanced techniques such as electron-beam lithography,^{11,12} interference lithography,¹³ and microcontact printing^{14–16} to spatially localize initiating species. Recently, methods such as surface-initiated electrochemical ATRP (eATRP)^{17–20} have been reported by several groups as versatile alternatives to traditional surface patterning procedures. While these techniques offer notable improvements in the field, they also pose certain challenges, including delayed response time for complete deactivation, requirement for copper-based catalysts, and the lack of easy access to arbitrarily patterned surfaces.²¹

In addressing these challenges, our group reported a light-mediated ATRP process using an Ir-based photoredox catalyst^{22–24} to spatially and temporally control polymer

brush synthesis from uniformly functionalized initiating layers.²⁵ The key to the success of this method is the use of light as a mild, noninvasive stimulus for selective polymer growth, allowing access to three-dimensional nanostructures in a single step. While this process provides a significant advancement in patterned polymer brush fabrication, the need for a metal catalyst remains problematic for a number of applications in areas such as microelectronics and bioinspired materials.^{26,27} Heavy metal-based marine antifouling coatings serve as a prime example, as bioaccumulation of released metal ions in the environment is known to harm wildlife.^{28,29} As a result, significant effort has been exerted to develop systems with decreased catalyst loadings^{30–32} as well as improved postprocess purification of trace metals.^{33–35} Additionally, the very high cost of Ir(ppy)₃ (\$1080/g) coupled with rigorous deoxygenation procedures (multiple freeze–pump–thaw steps) make implementation on a large scale impractical and therefore greatly hinder their development and application.³⁶

Drawing inspiration from recent developments in photocontrolled living radical polymerizations,³⁷ such as phenothiazine-based metal-free ATRP,³⁸ and its observed oxygen tolerance in small molecule dehalogenations,³⁹ we sought to develop a metal-free, benchtop system for the preparation of surface-tethered polymer brushes (Figure 1). This straightfor-

Received: January 4, 2016

Accepted: January 29, 2016

Published: February 2, 2016

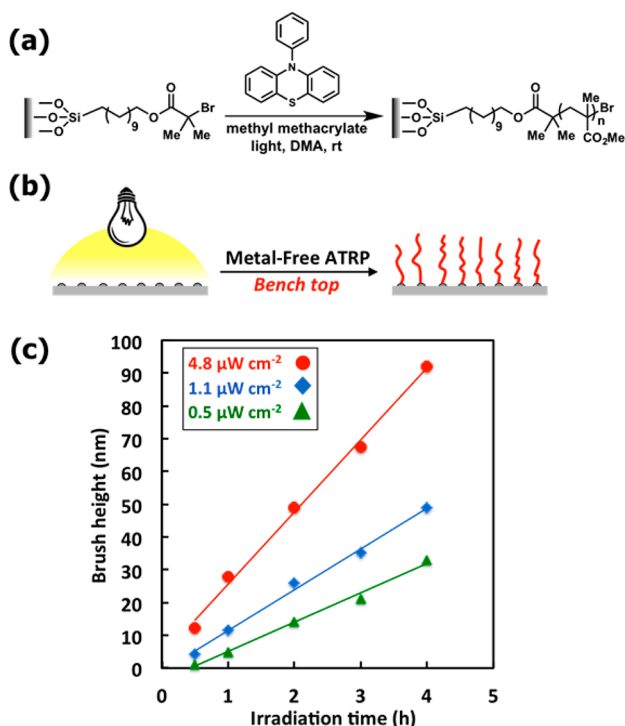


Figure 1. (a) Chemical scheme and conditions for metal-free ATRP using α -bromoisobutyrate-based initiator-functionalized silicon substrates. (b) Illustration of surface-initiated, metal-free ATRP (c) Plot of brush height as a function of irradiation time using varied light intensities in the benchtop chamber.

ward procedure involves the use of a modified Petri dish with a covering glass slide, allowing for top-down irradiation of surfaces (see SI, Figure S2). Well-defined single-layer patterns, gradient structures, and block copolymer architectures are readily available using traditional binary and/or grayscale photomasks. The use of irradiation from commercially available light sources, including compact fluorescent lamps (CFLs) and even natural sunlight, further simplifies this process.

To understand the potential of this method, kinetic experiments were conducted to track the relationship between brush height and irradiation time. Using silicon substrates uniformly functionalized with α -bromoisobutyrate-based initiators (Figure 1a), a series of polymerizations to prepare poly(methyl methacrylate) (PMMA) brushes were performed using irradiation with visible light ($\lambda = 405$ nm) at a range of intensities for varied lengths of time (Figure 1c). After thorough washing, thicknesses were measured using optical reflectometry, and a linear relationship between brush height and irradiation time was observed for each of the intensities investigated. As a control, an analogous series of experiments using $1.1 \mu\text{W/cm}^2$ intensity light were performed in an inert glovebox environment, yielding comparable results to the benchtop system (see SI, Figure S4).

After observing a linear increase in brush height, the ability of phenothiazine-mediated SI-ATRP to grow diblock copolymers was explored. Thus, a uniform PMMA brush was first prepared under optimized conditions and measured to be 30 nm. Following this, a diblock copolymer was synthesized via chain extension with 2,2,2-trifluoroethyl methacrylate (TFEMA) (Figure 2). Optical reflectometry measurements indicated an increase in overall brush thickness of approximately 26 nm, suggesting retention of active chain ends. Moreover, character-

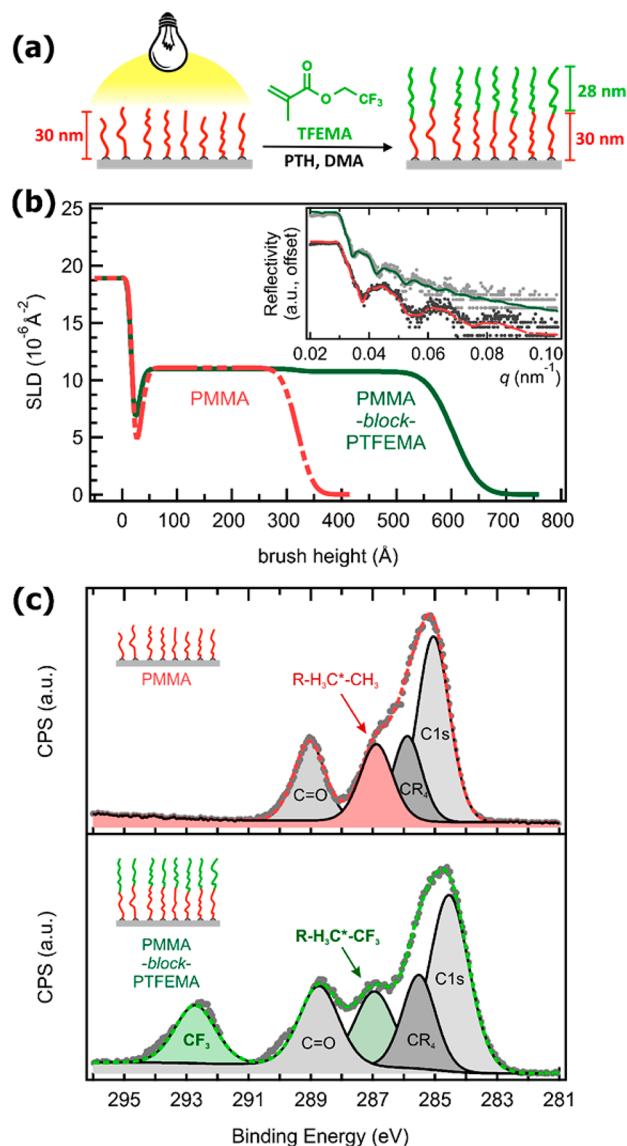


Figure 2. (a) Metal-free SI-ATRP preparation of uniform diblock copolymers via chain extension of PMMA, with brush heights measured by optical reflectometry. (b) X-ray reflectivity (XRR) data illustrate an increase in film thickness from the initial block. Raw data and fitting are shown in the inset. (c) X-ray photoelectron spectroscopy (XPS) plots show the emergence of characteristic signals of covalently bound fluorine found in the PTFEMA block.

ization by X-ray reflectivity (XRR) revealed a collapse of refractive fringes (Figure 2b, inset) corresponding to thicknesses that match those obtained by optical reflectometry. Scattering length densities (Figure 2b) were fitted via a three- and four-layer model for the PMMA homopolymer and diblock copolymer brushes, respectively, further confirming the increase in brush thickness after block copolymer formation. Additional characterization by X-ray photoelectron spectroscopy (XPS) reaffirmed diblock copolymer composition, with the emergence of a fluorine–CF₃ peak at 292.72 eV (Figure 2c). These results suggest that chain extension is achievable when performing benchtop ATRP with *N*-phenyl phenothiazine as the catalyst.

A profound advantage of light-mediated surface polymerization is the ability to exert direct spatial control over brush growth using readily available photomasks with arbitrary patterns.⁴⁰ Using the benchtop setup, a binary photomask

containing discrete line features with spacings down to $2\ \mu\text{m}$ (Figure 3b), as well as various polygonal structures down to 1

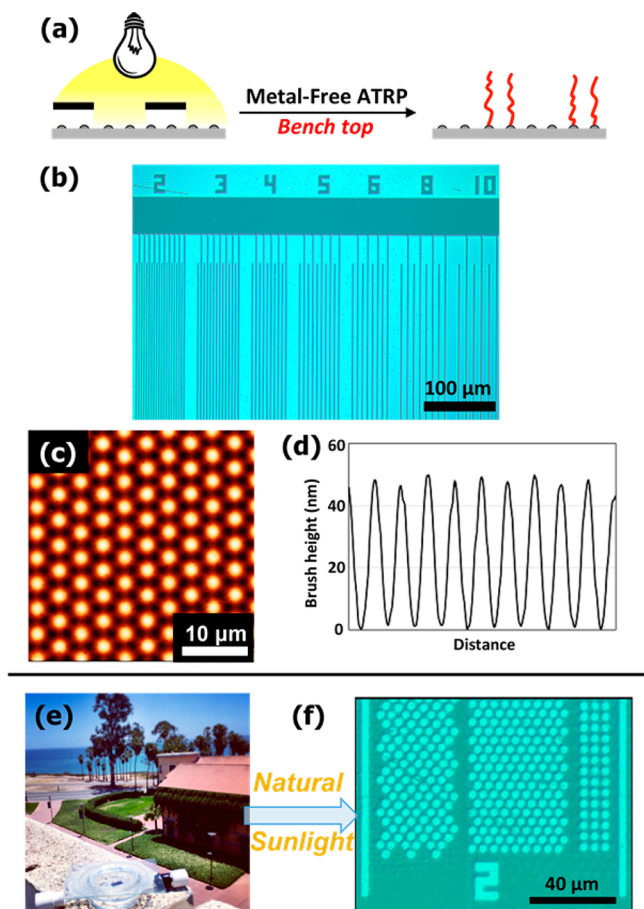


Figure 3. (a) Binary photomasks enable one-step patterning. (b) Optical micrograph of micron-scale line features ($2\text{--}10\ \mu\text{m}$). (c) AFM image of $1\ \mu\text{m}$ features and (d) corresponding AFM height profile. (e) Polymerization using sunlight and (f) optical micrograph of patterned $2\ \mu\text{m}$ features (see SI for setup).

μm , was placed over a silicon substrate and irradiated using optimized conditions. After 3 h, well-defined patterning was observed by optical microscopy. Characterization by AFM revealed highly uniform patterning for $1\ \mu\text{m}$ features (Figure 3c and d). Experiments were then conducted using a grayscale photomask to demonstrate the facile production of complex gradient structures (see SI, Figure S6). A well-defined gradient was observed, exemplifying the ability of metal-free SI-ATRP to prepare arbitrary patterns on surfaces.

In order to further highlight the capabilities of the benchtop setup, a polymerization was then conducted under natural sunlight. With no additional precautions, the reaction was performed by placing the apparatus in direct sunlight for 4 h, and after thorough washing, well-defined patterns were observed (Figure 3e and f). This offers a significant advantage over previous light-mediated systems, which were limited to the glovebox, and further demonstrates the modularity and ease of phenothiazine-mediated, metal-free SI-ATRP.

As an additional example of modularity, we investigated the application of this methodology to a larger-scale surface (i.e., four-inch diameter silicon wafer). This use is of particular interest as there are few reports of using SI-ATRP for polymer brush synthesis on large-scale wafers.⁴¹ When reported, these

methods do not allow for well-defined spatial control. Using the benchtop chamber, an initiator-functionalized four-inch wafer was patterned using a binary photomask with irradiation from a commercially available compact fluorescent lamp (see SI, Figure S9). Arbitrary micron-scale patterns, as well as millimeter-scale patterns were all obtained in a single step (Figure 4), reaffirming the potential of metal-free SI-ATRP for large-scale wafer applications.

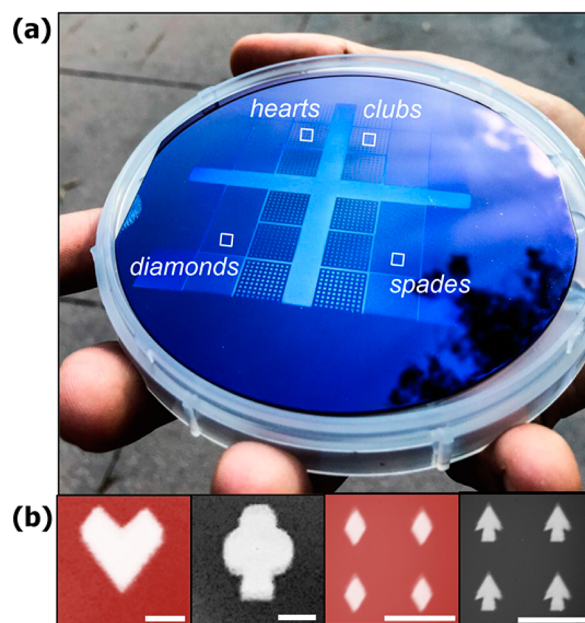


Figure 4. (a) Photograph of large area patterning in a single step of a four-inch wafer using a binary photomask. (b) Optical micrographs of patterned arbitrary features. Scale bars are $200\ \mu\text{m}$.

For patterning diblock copolymer architectures, the ability to achieve selective initiation from existing homopolymer brushes is particularly powerful as it enables the fabrication of diverse, spatially defined structures. Much like the experiments used to obtain uniform diblocks, analogous experiments were conducted using a binary photomask containing various micron-scale features. First, a uniform homopolymer layer of $38\ \text{nm}$ was prepared using 2-(methylthio)ethyl methacrylate (MTEMA) as the monomer. After washing, a subsequent chain extension experiment was conducted using TFEMA with irradiation through a binary photomask to achieve high-fidelity PMTEMA-*b*-PTFEMA diblock copolymer patterns (Figure 5). In addition to characterization by optical microscopy, dynamic secondary ion mass spectrometry (SIMS) was implemented to chemically map the patterned brush surface. Indeed when the ^{19}F signal was scanned, a micron-scale pattern of the PTFEMA layer can be clearly observed. Moreover, an inverse pattern is obtained when scanning for the ^{32}S signal found in the starting PMTEMA brush (^{19}F -containing layer masks the underlying ^{32}S signal). As a ^{12}C reference scan of the entire brush region shows a continuous brush layer, the patterning must be due to the presence of domains of fluorinated blocks on an underlying brush layer as depicted graphically in Figure 5a (see also SI, Figure S10). Furthermore, analogous SIMS results were obtained for patterned PMMA-*b*-PTFEMA copolymer brushes (see SI, Figure S11), demonstrating that efficient patterning occurs for a number of polymer systems. These data thoroughly

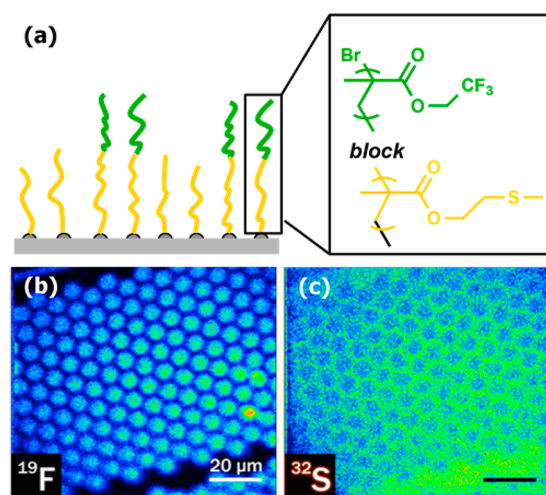


Figure 5. (a) Schematic of PMTEMA-*b*-PTFEMA patterned surfaces. (b) Dynamic secondary ion mass spectroscopy (SIMS) image of patterned fluorine signal from PTFEMA. (c) SIMS image of patterned sulfur signal from PMTEMA.

support the ability to achieve high fidelity spatially controlled reinitiation of chain ends with metal-free SI-ATRP.

Encouraged by the results obtained on silicon wafers, it was next sought to extend metal-free SI-ATRP to curved surfaces, such as silica nanoparticles. The field of surface modification of nanoparticles with polymer brushes has seen growing interest due to the resulting properties of well-defined core-shell architectures, with applications in optics, magnetics, electronics, and drug delivery.^{7,42} We envisioned potentially furthering the scope of these applications by taking advantage of a metal-free approach to these materials, as well as offering a system that would not require tedious purification steps.

To illustrate the versatility of this approach and the ability to grow brushes from particle surfaces in solution, commercially available silica nanoparticles were functionalized with α -bromoisobutyrate-based ATRP initiators. The nanoparticles were subsequently subjected to light-mediated, solution-based conditions in the presence of *N*-phenyl phenothiazine as catalyst (see SI). After 4 h of irradiation, the particles were purified via rigorous washing and centrifugation steps. Next, attenuated total reflectance-Fourier transform infrared (ATR-FTIR) spectroscopy was used to analyze and compare the PMMA-functionalized particles to the bare and initiator bound particles. The results for the SiO₂-PMMA nanoparticles showed the emergence of a peak at 1725 cm⁻¹, representative of carbonyl groups present in the PMMA backbone (Figure 6a). Moreover, transmission electron microscopy (TEM) was used to image the dried SiO₂ nanoparticles, and a clear PMMA shell was observed (Figure 6c,d), the thickness of which correlates with the mass loss obtained by TGA (see SI). Thermogravimetric analysis (TGA) of the polymer-grafted nanoparticles compared to the bare and initiator-functionalized nanoparticles clearly showed a greater weight loss for the PMMA-functionalized nanoparticles (see SI, Figure S12). Subsequent analysis of cleaved polymers by ¹H NMR and gel permeation chromatography (GPC) also further supported the presence of PMMA (see SI, Figure S13). These results are promising preliminary evidence showing the versatility of visible-light-mediated SI-ATRP for the synthesis of polymer brushes across a wide range of surfaces and reaction conditions.

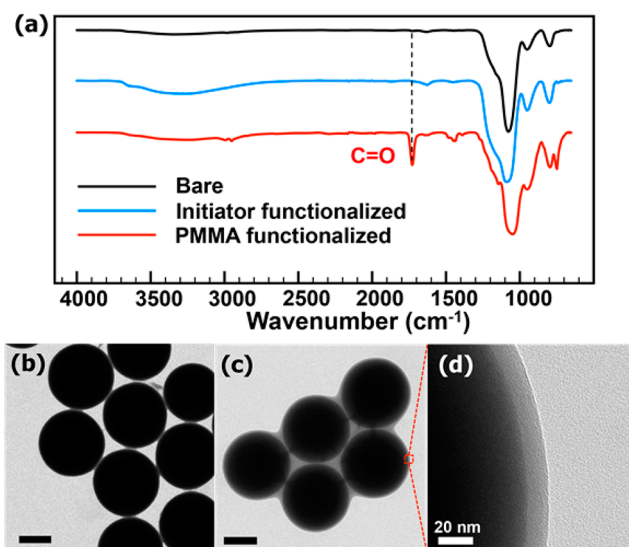


Figure 6. (a) ATR-FTIR showing the emergence of the carbonyl signal at 1725 cm⁻¹ for PMMA-functionalized SiO₂ nanoparticles versus bare and initiator-functionalized particles. (b) TEM of bare SiO₂ nanoparticles. (c) TEM image of PMMA-functionalized core-shell SiO₂ nanoparticles. (d) Magnification of PMMA-functionalized SiO₂ nanoparticles (scale bars are 200 nm unless otherwise noted).

In conclusion, a robust and versatile benchtop method for the fabrication of surface-tethered polymer brushes using light-mediated, metal-free ATRP on both wafers and nanoparticles has been demonstrated. Utilizing an inexpensive organic phenothiazine-based photocatalyst in combination with a simplified benchtop reaction chamber and readily available visible-light sources, spatially controlled brush growth was demonstrated, even on large 4 in. wafer surfaces. Investigation of monomer scope and extension of synthetic versatility of this system for the preparation of increasingly complex functional materials on a wide array of surfaces are currently underway.

■ ASSOCIATED CONTENT

Supporting Information

The Supporting Information is available free of charge on the ACS Publications website at DOI: 10.1021/acsmacrolett.6b00004.

General reagent information, general analytical information, light sources, synthesis of 10-phenylphenothiazine, synthesis of uniformly functionalized alkyl bromide silicon surfaces, attachment of alkyl bromide initiator to surface, catalyst loading experiments, irradiation time vs brush height experiments, irradiation time vs brush height experiments, and additional experimental details (PDF)

■ AUTHOR INFORMATION

Corresponding Authors

*E-mail: hawker@mrl.ucsb.edu.

*E-mail: javier@chem.ucsb.edu.

Notes

The authors declare no competing financial interest.

■ ACKNOWLEDGMENTS

We thank the MRSEC program of the National Science Foundation (DMR 1121053, C.J.H., J.R.A.) and The Dow

Chemical Company through the Dow Materials Institute at UCSB (E.H.D., N.J.T., C.W.P., B.N., K.M.M., E.T., J.L., Y.L., A.J.M., C.J.H., J.R.A.) for financial support. E.H.D., N.J.T. and K.M.M. thank the NSF Graduate Research Fellowship, and C.W.P. acknowledges the Alexander von Humboldt Foundation for financial support. K.M.M., B.N., and C.J.H. also acknowledge the PREM program of the National Science Foundation (DMR-1205194) for support. We sincerely thank Richard Bock for the fabrication of the benchtop chamber, David Bothman and Lee Sawyer for photomask fabrication, Thomas Mates for SIMS imaging, and Amanda Strom and Rachel Behrens for help with polymer characterization.

REFERENCES

- (1) Barbey, R.; Lavanant, L.; Paripovic, D.; Schüwer, N.; Sugnaux, C.; Tugulu, S.; Klok, H.-A. *Chem. Rev.* **2009**, *109*, 5437–5527.
- (2) (a) Husseman, M.; Malmström, E. E.; McNamara, M.; Mate, M.; Mecerreyes, D.; Benoit, D. G.; Hedrick, J. L.; Mansky, P.; Huang, E.; Russell, T. P.; Hawker, C. J. *Macromolecules* **1999**, *32*, 1424–1431. (b) Devonport, W.; Michalak, L.; Malmstrom, E.; Mate, M.; Kurdi, B.; Hawker, C. J.; Barclay, G. G.; Sinta, R. *Macromolecules* **1997**, *30*, 1929–1934.
- (3) Baum, M.; Brittain, W. J. *Macromolecules* **2002**, *35*, 610–615.
- (4) Pyun, J.; Jia, S.; Kowalewski, T.; Patterson, G. D.; Matyjaszewski, K. *Macromolecules* **2003**, *36*, 5094–5104.
- (5) Matyjaszewski, K.; Miller, P. J.; Shukla, N.; Immaraporn, B.; Gelman, A.; Luokala, B. B.; Siclován, T. M.; Kickelbick, G.; Vallant, T.; Hoffmann, H.; Pakula, T. *Macromolecules* **1999**, *32*, 8716–8724.
- (6) Dalsin, J. L.; Hu, B.-H.; Lee, B. P.; Messersmith, P. B. *J. Am. Chem. Soc.* **2003**, *125*, 4253–4258.
- (7) Krishnamoorthy, M.; Hakobyan, S.; Ramstedt, M.; Gautrot, J. E. *Chem. Rev.* **2014**, *114*, 10976–11026.
- (8) Sun, G.; Cho, S.; Yang, F.; He, X.; Pavia-Sanders, A.; Clark, C.; Raymond, J. E.; Verkhoturov, S. V.; Schweikert, E. A.; Thackeray, J. W.; Trefonas, P.; Wooley, K. L. *J. Polym. Sci., Part A: Polym. Chem.* **2015**, *53*, 193–199.
- (9) Stuart, M. A. C.; Huck, W. T. S.; Genzer, J.; Müller, M.; Ober, C.; Stamm, M.; Sukhorukov, G. B.; Szleifer, I.; Tsukruk, V. V.; Urban, M.; Winnik, F.; Zauscher, S.; Luzinov, I.; Minko, S. *Nat. Mater.* **2010**, *9*, 101–113.
- (10) Sun, L.; Baker, G. L.; Bruening, M. L. *Macromolecules* **2005**, *38*, 2307–2314.
- (11) Ballav, N.; Schilp, S.; Zharnikov, M. *Angew. Chem., Int. Ed.* **2008**, *47*, 1421–1424.
- (12) Khan, M. N.; Tjong, V.; Chilkoti, A.; Zharnikov, M. *Angew. Chem., Int. Ed.* **2012**, *51*, 10303–10306.
- (13) Schuh, C.; Santer, S.; Prucker, O.; Ruhe, J. R. *Adv. Mater.* **2009**, *21*, 4706–4710.
- (14) Zhou, F.; Zheng, Z.; Yu, B.; Liu, W.; Huck, W. T. S. *J. Am. Chem. Soc.* **2006**, *128*, 16253–16258.
- (15) Azzaroni, O.; Moya, S. E.; Brown, A. A.; Zheng, Z.; Donath, E.; Huck, W. T. S. *Adv. Funct. Mater.* **2006**, *16*, 1037–1042.
- (16) Li, B.; Yu, B.; Ye, Q.; Zhou, F. *Acc. Chem. Res.* **2015**, *48*, 229–237.
- (17) Li, B.; Yu, B.; Huck, W. T. S.; Zhou, F.; Liu, W. *Angew. Chem., Int. Ed.* **2012**, *51*, 5092–5095.
- (18) Shida, N.; Koizumi, Y.; Nishiyama, H.; Tomita, I.; Inagi, S. *Angew. Chem., Int. Ed.* **2015**, *54*, 3922–3926.
- (19) Yan, J.; Li, B.; Yu, B.; Huck, W. T. S.; Liu, W.; Zhou, F. *Angew. Chem., Int. Ed.* **2013**, *52*, 9125–9129.
- (20) Li, B.; Yu, B.; Huck, W. T. S.; Liu, F. W.; Zhou, F. *J. Am. Chem. Soc.* **2013**, *135*, 1708–1710.
- (21) (a) Leibfarth, F. A.; Mattson, K. M.; Fors, B. P.; Collins, H. A.; Hawker, C. J. *Angew. Chem., Int. Ed.* **2013**, *52*, 199–210. (b) Hadadpour, M.; Ragogna, P. J. *J. Polym. Sci., Part A: Polym. Chem.* **2015**, *53*, 2747–2754.
- (22) (a) Fors, B. P.; Hawker, C. J. *Angew. Chem., Int. Ed.* **2012**, *51*, 8850–8853. (b) Treat, N. J.; Fors, B. P.; Kramer, J. W.; Christianson, M.; Chiu, C.-Y.; Alaniz, J. R. de; Hawker, C. J. *ACS Macro Lett.* **2014**, *3*, 580–584.
- (23) Yamago, S.; Nakamura, Y. *Polymer* **2013**, *54*, 981–994.
- (24) Pester, C. W.; Poelma, J. E.; Narupai, B.; Patel, S. N.; Su, G. M.; Mates, T. E.; Luo, Y.; Ober, C. K.; Hawker, C. J.; Kramer, E. J. *J. Polym. Sci., Part A: Polym. Chem.* **2016**, *54*, 253–262.
- (25) Poelma, J. E.; Fors, B. P.; Meyers, G. F.; Kramer, J. W.; Hawker, C. J. *Angew. Chem., Int. Ed.* **2013**, *52*, 6844–6848.
- (26) Ouchi, M.; Terashima, T.; Sawamoto, M. *Chem. Rev.* **2009**, *109*, 4963–5050.
- (27) Matyjaszewski, K.; Tsarevsky, N. V. *J. Am. Chem. Soc.* **2014**, *136*, 6513–6533.
- (28) Yang, W. J.; Neoh, K.-G.; Kang, E.-T.; Teo, S. L.-M.; Rittschof, D. *Prog. Polym. Sci.* **2014**, *39*, 1017–1042.
- (29) Chambers, L. D.; Stokes, K. R.; Walsh, F. C.; Wood, R. J. K. *Surf. Coat. Technol.* **2006**, *201*, 3642–3652.
- (30) Kwak, Y.; Magenau, A. J. D.; Matyjaszewski, K. *Macromolecules* **2011**, *44*, 811–819.
- (31) Gnanou, Y.; Hizal, G. J. *J. Polym. Sci., Part A: Polym. Chem.* **2004**, *42*, 351–359.
- (32) Magenau, A. J. D.; Strandwitz, N. C.; Gennaro, A.; Matyjaszewski, K. *Science* **2011**, *332*, 81–84.
- (33) Shen, Y.; Zhu, S. *Macromolecules* **2001**, *34*, 8603–8609.
- (34) Munirasu, S.; Aggarwal, R.; Baskaran, D. *Chem. Commun.* **2009**, *30*, 4518–3.
- (35) Matyjaszewski, K.; Pintauer, T.; Gaynor, S. *Macromolecules* **2000**, *33*, 1476–1478.
- (36) Azzaroni, O. *J. Polym. Sci., Part A: Polym. Chem.* **2012**, *50*, 3225–3258.
- (37) Ohtsuki, A.; Lei, L.; Tanishima, M.; Goto, A.; Kaji, H. *J. Am. Chem. Soc.* **2015**, *137*, 5610–5617.
- (38) (a) Treat, N. J.; Sprafke, H.; Kramer, J. W.; Clark, P. G.; Barton, B. E.; Read de Alaniz, J.; Fors, B. P.; Hawker, C. J. *J. Am. Chem. Soc.* **2014**, *136*, 16096–16101. (b) Pan, X.; Lamson, M.; Yan, J.; Matyjaszewski, K. *ACS Macro Lett.* **2015**, *4*, 192–196.
- (39) Discekici, E. H.; Treat, N. J.; Poelma, S. O.; Mattson, K. M.; Hudson, Z. M.; Luo, Y.; Hawker, C. J.; de Alaniz, J. R. *Chem. Commun.* **2015**, *51*, 11705.
- (40) Chen, T.; Amin, I.; Jordan, R. *Chem. Soc. Rev.* **2012**, *41*, 3280.
- (41) Zhang, T.; Du, T.; Kalbakova, J.; Schubel, R.; Rodrigues, R. D.; Chen, T.; Zahn, D.; Jordan, R. *Polym. Chem.* **2015**, *6*, 8176–8183.
- (42) Wu, L.; Glebe, U.; Böker, A. *Polym. Chem.* **2015**, *6*, 5143–5184.